Whispering-gallery mode terahertz pulses

Jiangquan Zhang and D. Grischkowsky

School of Electrical and Computer Engineering and Center for Laser and Photonics Research, Oklahoma State University, Stillwater, Oklahoma 74078

Received November 13, 2001

We report what is to our knowledge the first observation of a subpicosecond terahertz (THz) pulse propagating as a superposition of the whispering-gallery modes (WGMs) of a dielectric cylinder. The WGM THz pulses are coupled into and out of a 5-mm-diameter silicon cylinder via a 100-μm-thick, single-mode silicon slab waveguide. We observed two round-trip cylindrical cavity pulses from this coupling structure, which cover a continuous frequency range from 0.4 to 1.8 THz. The coupled-mode equations are used to analyze this system and give reasonably good agreement with the experiment in both the frequency and the time domains.

OCIS codes: 230.0230, 250.0250.

The optical cavity has attracted considerable research interest because of its important applications in laser design,[1] cavity-ringdown spectroscopy,[2] fiber optics,[3] and basic research such as cavity quantum electrodynamics.[4] In the microwave region, spherical or cylindrical dielectric cavity resonators have been proved practical for high-performance frequency filters for millimeter-wave integrated circuits.[5] Recently an experimental demonstration of a broadband, quasi-optic dielectric terahertz (THz) cavity coupled through optical tunneling was reported.[6]

The whispering-gallery mode (WGM) is starting to play an important role in optical and microwave cavities. These modes, which occur in dielectric spheres and cylinders, describe electromagnetic radiation circulating about the inner surface of the cavity. Because of the total internal reflection associated with these modes, they can have cavity Q values that exceed 10^{10}. Consequently, WGM cavities are becoming important for ultranarrow linewidth, high-energy densities, and sensing applications. In addition, WGM cavities (resonators) offer adaptability to integrated circuits, which can provide excellent frequency selection for both millimeter[5] and optical[7,8] waves.

In this Letter we report what we believe is the first observation of a subpicosecond (subps) THz pulse propagating as a superposition of WGM modes of a dielectric cylinder. This observation is made possible by efficient coupling between a single-mode dielectric slab waveguide[9] and a dielectric cylindrical WGM resonator for THz pulses. Unlike the related WGM studies of microspheres that use single-frequency cw optical lasers,[7,8] here we use subps THz pulses.[9] The coupled WGM pulse covers a continuous frequency range from 0.4 to 1.8 THz and consists of a superposition of several WGM modes. The experimental results thereby have demonstrated the WGM propagation properties and the strong coupling between the slab waveguide and the cylinder.

The experimental setup is similar to that which has been used to investigate THz propagation in plastic ribbon waveguides[9] and incorporates plano–cylindrical lenses to couple the energy into and out of the slab guide. The slab waveguide and the cylinder are both made from high-resistivity silicon, with dimensions of 17.5 mm (length z) by 100 μm (thickness x) by 12.5 mm (height y) and 5 mm (diameter) by 10 mm (height y), respectively. As illustrated in the center inset of Fig. 1, the slab waveguide is sandwiched between two 18-mm (length z) by 25 mm (height y) aluminum plates, each with a 3.2-mm (length z) by 17 mm (height y) open window in the middle. To place the cylinder in contact with the slab waveguide we carefully milled out the open window of the bottom plate, using a 6.2-mm ball-end bit. A 5-mm aperture was placed before the left lens to confine the incoming beam.

Figure 1 shows the measured THz pulses of the system described above. Pulse 1a is the reference scan taken without the cylinder and is the main transmitted pulse, which is followed by two smaller pulses, 2a and 3a, that are due to reflections from the cylindrical lenses. When the cylinder is brought into contact with the slab waveguide, two new pulses, 4b and 5b, appear, as shown in Fig. 1(b).

The x-polarized input subps THz pulse, which we measured by removing the coupling structure and moving the cylindrical lenses to their confocal position,[9,10] is shown in the left inset of Fig. 1. This pulse is coupled with good efficiency into the TEM mode of the parallel-plate metal waveguide formed by the two aluminum plates. The TEM THz pulse propagates with negligible distortion and loss,[10] except in the window region, where it propagates in the slab TM_0 mode with high group-velocity dispersion, which causes the extreme broadening and frequency chirp of pulses 1a, 2a, and 3a (Fig. 1).[9] For Fig. 1(b), when the THz pulse reaches the slab–cylinder contact region, part of the pulse will be coupled into the cylinder as a linear combination of WGM modes; the remaining pulse continues to propagate along the beam path of the system and is detected as the main transmitted pulse, 1b. The WGM THz pulse travels continuously about the cylinder. When it returns to the slab–cylinder contact region after one round trip, part of this pulse is coupled into the slab waveguide and arrives at the THz receiver to be recorded as the first cavity pulse 4b. As this coupling occurs every time the circulating

0146-9592/02/080661-03$15.00/0

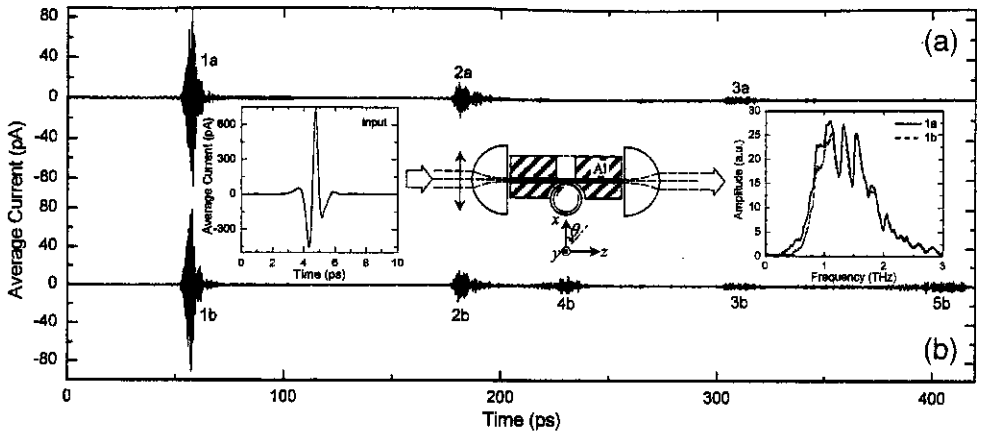

Fig. 1. Measured time-domain pulses. (a) Reference scan without the cylinder, (b) sample scan with the cylinder in contact with the slab waveguide. Rightmost inset, spectra of the main transmitted pulses for both situations. The measured input pulse is shown in the leftmost inset. The center inset shows the cross section of the slab–cylinder coupling structure.

WGM THz pulse returns to the contact region, a cavity pulse train is generated.

If we assume that the WGM THz pulse travels about the cylinder at a velocity equal to that in bulk silicon, the time delay between the first cavity pulse, 4b, and the main pulse, 1b, can be calculated as $\tau_1 = 2\pi n_c \rho / c$, where $n_c = 3.42$ is the refractive index of silicon, ρ is the radius of the cylinder, and c is the speed of light. Substituting the corresponding values, we get $\tau_1 = 179$ ps, in agreement with the experimental value of 172–187 ps. The observed delay of the second cavity pulse, 5b, with respect to pulse 1b is in the range 337–367 ps, in agreement with the calculated value of $\tau_2 = 2\tau_1 = 358$ ps.

Figures 2(a) and 2(b) are magnifications of Fig. 1 for the first and the second cavity pulses, 4b and 5b, respectively. Their respective spectra are presented in Figs. 3(a) and 3(b). The rightmost inset of Fig. 1 shows the spectra of single-mode main pulses 1a and 1b; the spectral oscillations are due to the reflections between the planar surfaces of the cylindrical lenses and the entrance and exit surfaces of the slab waveguide, separated by approximately 0.7 mm. However, the spectral oscillations of the cavity pulses shown in Fig. 3 indicate the multimode composition[11] of the WGM THz pulse; the oscillations occur because the phase velocities are different for the individual WGM modes and interference occurs when the pulses are coherently combined at the coupling point.

For single-mode coupling the frequency-domain coupled-mode equations that govern the coupling between the slab waveguide and the cylinder can be written as[12]

$$\frac{\mathrm{d}}{\mathrm{d}\theta}(P_{aa}a + P_{ab}b) = iC_{aa}a + iC_{ab}b\,, \tag{1a}$$

$$\frac{\mathrm{d}}{\mathrm{d}\theta}(P_{ba}a + P_{bb}b) = iC_{ba}a + iC_{bb}b\,, \tag{1b}$$

where a and b are the complex modal amplitudes for the slab and the WGM modes, respectively, and P and C are the coupling coefficients.[12] If we now assume that the transfer function of the main transmitted pulse, 1a, is $H_0(\omega)$, its complex spectrum will be $A_0(\omega) = H_0(\omega)I(\omega)$, where $I(\omega)$ is the complex spectrum of the input pulse. Similarly, the complex spectra of the output cavity pulses can be written as $A_m(\omega) = H_m(\omega)H_0(\omega)I(\omega)$, where for the first two cavity pulses ($m = 1, 2$) the transfer functions are given by

$$H_1(\omega) = \sum_n b_n{}^s(\omega)a_n{}^c(\omega)\exp[i2\pi l_n(\omega)]\,, \tag{2a}$$

$$H_2(\omega) = \sum_n b_n{}^s(\omega)b_n{}^c(\omega)a_n{}^c(\omega)\exp[i4\pi l_n(\omega)]\,. \tag{2b}$$

The subscript n indicates a particular WGM mode; $l_n(\omega)$ is the corresponding angular propagation constant[13]; $b_n{}^s$ [calculated from Eq. (1)] gives the complex amplitude coupling into the nth mode from the slab

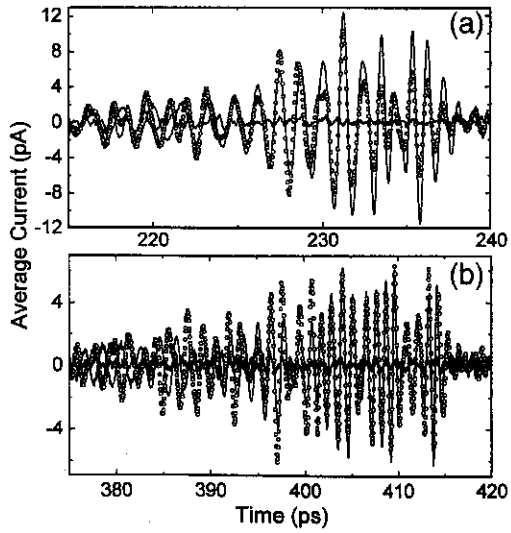

Fig. 2. Measured and calculated results of (a) the first (pulse 4b; Fig. 1) and (b) the second (pulse 5b) cavity pulses. Thin solid curves, references; curves with open circles, experiment; thick solid curves, calculation results.

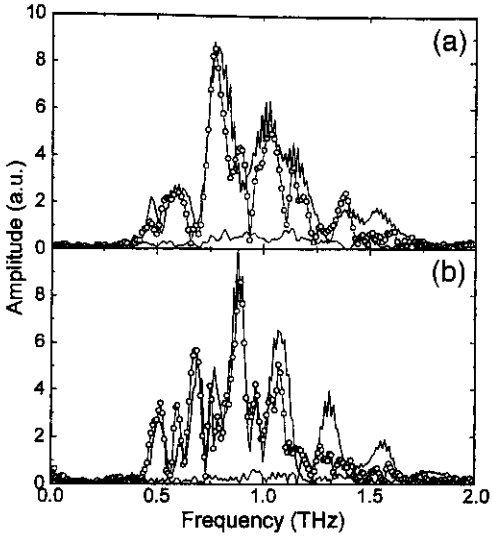

Fig. 3. Spectra of (a) the first (pulse 4b; Fig. 1) and (b) the second (pulse 5b) cavity pulses. Thin solid curves, references; curves with open circles, experimental results; thick solid curves, calculation results.

TM_0 mode; a_n^c is the coupling into the slab mode from the nth WGM mode, and b_n^c is the remaining complex amplitude of the nth mode in the cylinder after the first cavity pulse. Thus, given noncoupled THz pulse 1a through the slab waveguide, we can calculate the cavity pulses in both the frequency and the time domains.

In the calculation we assume that both the slab and the cylinder are longitudinally infinite and that, owing to the x polarization of the incoming THz beam, only the TM WGM modes are coupled into the cylinder. The numerical calculations presented in Figs. 2 and 3 include the coupling results for the first eight TM WGM modes. As can be seen for pulse 4b, initially the theoretical oscillation is too slow. However, at ~225 ps, synchronization is obtained, and the complicated experimental structure is then in excellent agreement with theory. For pulse 5b, initially the theory is out of phase with the experimental oscillation. Starting at ~395 ps, excellent agreement between experimental and theoretical oscillations is obtained, although many experimental maxima are significantly larger than in theory. Even though the experimental results in Fig. 3(a) show sharper and deeper interference minima than predicted by theory, the overall structures in both Figs. 3(a) and 3(b) are in reasonable agreement with theory.

The discrepancies between theory and experiment are considered to be due to limitations in the numerical calculations. The observed rapidly oscillating structures in both the time and the frequency domains involve constructive and destructive interference among the first eight WGM modes of the cylinder. This interference is determined by the complex product of coupling coefficients $b_n^s a_n^c$ and the relative phase difference between the WGM modes caused by propagation about the cylinder. For example, the relative phase difference at 1 THz that is due to propagating one time around the cylinder for the first two WGM modes is $(7.78)(2\pi)$ rad, which is approximately 5% of their total phase angle for this propagation. This result shows the sensitivity of the system, in which a small error in the total calculated phase can lead to a large error in the predicted interference. Consequently the numerical calculation for the WGM total phase angles must be performed to an accuracy of better than 0.1%.

In summary, this study has demonstrated the feasibility of using a slab–cylinder structure as an effective coupling scheme for a THz WGM cavity. Because the coupling source is a subps THz pulse instead of a cw wave, the coherence condition is not required for the coupled WGM modes; hence the cavity pulses cover a continuous frequency range rather than discrete frequency points. Clearly, this structure is an excellent choice for the study of propagation properties of single subps pulses of THz radiation propagating in the WGM modes of a cylinder. In addition, as recent progress in THz waveguide studies[9–11] has made possible the guided-wave propagation and circuit interconnection of THz radiation, this structure shows promise for use as a coupler and resonator for future THz integrated circuits.

This research was partially supported by the National Science Foundation and the U.S. Army Research Office. D. Grischkowsky's e-mail address is grischd@ceat.okstate.edu.

References

1. V. Sandoghdar, F. Treussart, J. Hare, V. Lefèvre-Seguin, J.-M. Raimond, and S. Haroche, Phys. Rev. A **54,** R1777 (1996).
2. A. C. R. Pipino, J. W. Hudgens, and R. E. Huie, Rev. Sci. Instrum. **68,** 2978 (1997).
3. M. Cai, O. Painter, and K. J. Vahala, Phys. Rev. Lett. **85,** 74 (2000).
4. S. Haroche and D. Kleppner, Phys. Today **42**(1), 24 (1989).
5. C. Vedrenne and J. Arnaud, IEE Proc. H **129,** 183 (1982).
6. W. L. Zhang, J. Q. Zhang, and D. Grischkowsky, Appl. Phys. Lett. **78,** 2425 (2001).
7. V. B. Braginsky, M. L. Gordetsky, and V. S. Ilchenko, Phys. Lett. A **137,** 393 (1989).
8. L. Collot, V. Lefèvre-Seguin, M. Brune, J. M. Raimond, and S. Haroche, Europhys. Lett. **23,** 327 (1993).
9. R. Mendis and D. Grischkowsky, J. Appl. Phys. **88,** 4449 (2000).
10. R. Mendis and D. Grischkowsky, Opt. Lett. **26,** 846 (2001).
11. G. Gallot, S. P. Jamison, R. W. McGowan, and D. Grischkowsky, J. Opt. Soc. Am. B **17,** 851 (2000).
12. Q. Han, Y. Kogami, Y. Tomabechi, and K. Matsumura, IEEE Trans. Microwave Theory Tech. **44,** 2017 (1996).
13. J. D. Stratton, *Electromagnetic Theory* (McGraw-Hill, New York, 1941).